Proceedings of ASME Turbo Expo 2011
GT2011
June 6-10, 2011, Vancouver, British Columbia, Canada

GT2011-45153

ON OCCURRENCE OF REVERSE FULL ANNULAR RUB

John J. Yu, Ph.D.
GE Energy
1631 Bently Parkway South
Minden, Nevada 89423 USA
Phone: (775) 215-1225
E-mail: john.yu@ge.com

ABSTRACT

This paper discusses reverse full annular rub based on a two degree-of-freedom rotor/seal model where a rubbing location can be simulated away from the lumped rotor mass. The analytical model is much closer to the experimental setup for comparison of results, and real machines for analysis, than the previous one degree-of-freedom model. Its closed-form solution is given including reverse rub amplitudes and relative phases as well as the normal contact force. The exact frequency equation in polynomial form yields reverse full annular rub frequencies without having to neglect any parameters. Many conclusions can be drawn directly from explicit expressions without numerical calculations. The solution with non-positive normal contact force indicates a dry-friction whirl/whip-free region, usually accompanied by low friction and/or high damping. The analytical study covers both dry-friction whirl and dry-friction whip, and their relations with dry friction factor, damping, and rotor speed. Range of reverse rub frequencies, their relation with rotor and rotor/seal coupled natural frequencies, and direction of frictional force, are also revealed. Destructive dry-friction whip experimental results are given which have fully confirmed the analytical formulas.

INTRODUCTION

Rubbing often occurs in rotating machines, due to tight seal clearance, changes in alignment condition, high unbalance response, etc. For many rubs in the field, the rotor only touches the seal during a fraction of its orbital motion. This type of malfunction is called partial rub, and typically opens the clearance a little bit higher without causing destructive damage to the machine. In full annular rub, however, the rotor maintains contact against the seal continuously. Forward precessional full annular rub is dependent on shaft speed and mass unbalance besides clearance, and orbits in the same direction of rotor speed, which typically would not cause destructive damages. Reverse precessional full annular rub, i.e., dry-friction whirl/whip, could occur at any speed for an unstable rotor/seal system if the rotor contacts the seal due to high synchronous vibration or impacts. This type of self-excited vibration, especially dry whip, may lead to a machine catastrophic failure.

Black [1] first examined forward precessional full annular rub with a model to include both rotor and stator masses along with their stiffness. The rubbing contact location was simplified to be in the same location as the lumped rotor mass. Black [2] then used the same model to investigate reverse full annular rub, and obtained dry-friction whirl range with U-shaped curve. However, the effect of damping was not included in his work. Crandall and Lingener [3-5] demonstrated dry-friction whirl and whip for very large clearance. Many of these results were also introduced by Childs [6] in his book. Yu and Bently [7-9] found that dry-friction whip could be generated spontaneously from forward rub without experiencing dry-friction whirl. Childs and Wilkes [10, 11] revisited Black's original work with inclusion of multiple rotor modes, and presented dry-friction whirl and whip experimental results.

This paper is to study the reverse full annular rub in a model more close to the experimental setup than that in the early work by Yu et al [7]. Rotor/seal contact is simulated away from the lumped rotor mass with a two degree-of-freedom model. Validity of the model then can be confirmed by good agreement between analytical and measured results. Obtained results are qualitatively in agreement with the pattern predicted by Black's simple model. The current work is able to match experimental results to show its value of modeling both qualitatively and quantitatively, and also to disclose some characteristics. The model shown with dimensions and

experimental data, together with its closed-form solution, serves as a reference for those who are interested in this area.

It is noticed that in Black's model, the contact part besides the rotor includes the whole stator or casing, even though the bearings supporting the rotor are within the casing. In this paper, the contact part besides the rotor includes only the seal part, which is attached to the casing in the same way as bearings. Dynamic deformation of the seal against the relatively rigid casing is considered as seal vibration amplitude. Therefore only mass, stiffness, and damping of the seal part are simulated as the contact part besides the rotor, not including the whole relatively rigid casing. The equations of motion and its solution would be in the exactly same form between these two approaches, except subscript "s" designated alternatively between "stator" and "seal".

ANALYTICAL MODEL

The equations of motion of the two-degree-of-freedom model can be given by:

$$M\ddot{\rho} + D\dot{\rho} + K_3\rho + K_2\left(\rho - \rho_r\right) = Mh\Omega^2 e^{j\Omega t} \tag{1}$$

and

$$M_s\ddot{\rho}_s + D_s\dot{\rho}_s + K_s\left(1 + j\eta_s\right)\rho_s + K_1\rho_r + K_2\left(\rho_r - \rho\right) = 0 \tag{2}$$

where $\rho = x + jy$ standing for rotor displacement at lumped mass location, $\rho_r = x_r + jy_r$ representing rotor displacement at seal location, $\rho_s = x_s + jy_s$ representing seal displacement, $j = \sqrt{-1}$, M and D are rotor mass and damping, K_1, K_2 and K_3 are stiffness among seal, rotor mass, and two support ends as shown in Fig. 1, M_s, D_s, η_s, and K_s are seal mass, damping, structural damping factor, and stiffness, h is the center of mass eccentricity, Ω is the rotor speed, and t is time. The gyroscopic effect is neglected in Eq. (1).

A contact force must exist between the rotor and the seal if a rub occurs. Denoting N as a normal contact force along with a friction factor μ yields the following equation:

$$K_1\rho_r + K_2\left(\rho_r - \rho\right) + N\left(1 + j\mu\right)\frac{\rho_r - \rho_s}{\left|\rho_r - \rho_s\right|} = 0 \tag{3}$$

Note that N is a scalar, not a complex variable. The force N acts from the seal to the rotor in the normal direction of the contact surface. The associated μN represents a sliding frictional force when μ reaches its upper limit and remains constant (dry-friction whip), or a rolling frictional force when μ is below its upper limit and may vary (dry-friction whirl).

To maintain a full annular rub, the following geometrical condition must be satisfied:

$$\left|\rho_r - \rho_s\right| = C_r \tag{4}$$

where C_r stands for radial clearance between the rotor and the seal.

$N > 0$ is a necessary condition to have rubbing, and will be used in later analysis. Slip velocity v_{slip} (defined to be positive if in the same direction as rotor speed) at the contact surface is given by

$$v_{slip} = r\Omega + C_r\omega = C_r\Omega\left(\frac{r}{C_r} + \frac{\omega}{\Omega}\right) \tag{5}$$

where r stands for radius of the rotor at the contact surface, and ω represents shaft whirling speed (defined to be positive if in the same direction as rotor speed). Certainly for reverse rub, $\omega < 0$. In the dry whip condition, the associated frictional force μN ($=\mu_{slip}N$ where μ_{slip} is slip friction factor) will be in the opposite direction to the rotor speed if $v_{slip} > 0$. In the case of dry whirl where slip velocity is zero, frictional factor is less than its upper limit (slip frictional factor), i.e., $\mu < \mu_{slip}$. Equation (3) does not limit the possibility of negative μ though this case is proofed to be impossible later.

Since mass unbalance has no effect of maintaining a reverse full annular rub [7], the right hand side of Eq. (1) is neglected. When such a reverse rub occurs with frequency ω, Eqs. (1) to (4) allow for response in the following form

$$\rho = Ae^{j(\omega t + \alpha)} \tag{6}$$

$$\rho_r = A_r e^{j(\omega t + \alpha_r)} \tag{7}$$

$$\rho_s = A_s e^{j(\omega t + \alpha_s)} \tag{8}$$

where A, A_r, A_s, and α, α_r, α_s, stand for amplitude and phase for ρ, ρ_r, ρ_s, respectively.

Inserting Eqs. (6) to (8) into Eqs. (1) to (4) yields

$$R(\omega) - K_2\frac{A_r}{A}e^{j(\alpha_r - \alpha)} = 0 \tag{9}$$

$$R_s(\omega)\frac{A_s}{A}e^{j(\alpha_s - \alpha)} + \left(K_1 + K_2\right)\frac{A_r}{A}e^{j(\alpha_r - \alpha)} - K_2 = 0 \tag{10}$$

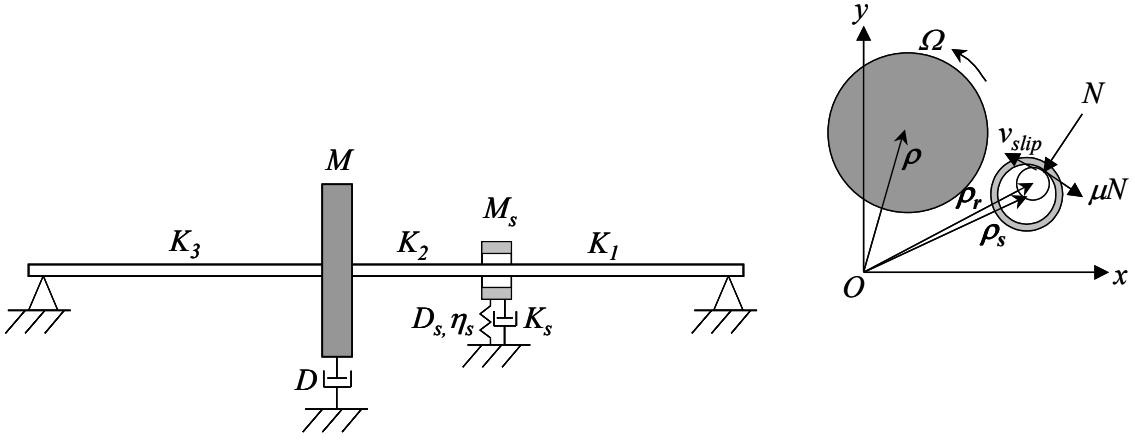

Figure 1. Diagram of analytical mode for reverse full annular rub

$$\left(K_1+K_2\right)\frac{A_r}{A}e^{j(\alpha_r-\alpha)}-K_2+ \\ +N\frac{1+j\mu}{C_r}\left[\frac{A_r}{A}e^{j(\alpha_r-\alpha)}-\frac{A_s}{A}e^{j(\alpha_s-\alpha)}\right]=0 \tag{11}$$

$$\left|A_r e^{j(\alpha_r-\alpha)}-A_s e^{j(\alpha_s-\alpha)}\right|=C_r \tag{12}$$

where

$$R(\omega)=K_2+K_3-\omega^2M+j\omega D \tag{13}$$

$$R_s(\omega)=K_s-\omega^2M_s+j\left(\omega D_s+K_s\eta_s\right) \tag{14}$$

Thus, the normal contact force N is given by

$$N=C_r\frac{1}{1+j\mu}R(\omega)\frac{\left(K_1+K_2\right)R(\omega)-K_2^2}{K_2^2-\left(K_1+K_2\right)R(\omega)-R(\omega)R_s(\omega)} \tag{15}$$

Since N is a scalar variable, its imaginary part should be zero, i.e.,

$$\mathrm{Im}(N)=0 \tag{16}$$

which is equivalent to the following expression:

$$\mu\left[a_1(\omega)+a_2(\omega)+a_3(\omega)\right]-\left[a_4(\omega)+a_5(\omega)\right]=0 \tag{17}$$

where

$$a_1(\omega)=\left(\omega^2-\omega_0^2\right)\left(\omega^2-\omega_s^2\right)\left(\omega^2-\omega_{c1}^2\right)\left(\omega^2-\omega_{c2}^2\right) \tag{18}$$

$$a_2(\omega)=\left(\frac{D_s}{M_s}\omega+\omega_s^2\eta_s\right)\left(\omega^2-\frac{K_2+K_3}{M}\right)\left(\omega^2-\omega_0^2\right) \tag{19}$$

$$a_3(\omega)=\left(\frac{D}{M}\right)^2\omega^2\left[\begin{array}{l}\left(\omega^2-\omega_s^2\right)\left(\omega^2-\dfrac{K_1+K_2+K_s}{M_s}\right)\\ +\left(\dfrac{D_s}{M_s}\omega+\omega_s^2\eta_s\right)^2\end{array}\right] \tag{20}$$

$$a_4(\omega)=\frac{DK_2^2}{\left(K_1+K_2\right)M^2}\omega\left[\left(\omega^2-\omega_s^2\right)^2+\left(\frac{D_s}{M_s}\omega+\omega_s^2\eta_s\right)^2\right] \tag{21}$$

$$a_5(\omega)=\frac{K_1+K_2}{M_s}\left(\frac{D_s}{M_s}\omega+\omega_s^2\eta_s\right)\left[\left(\omega^2-\omega_0^2\right)^2+\left(\frac{D}{M}\right)^2\omega^2\right] \tag{22}$$

with

$$\omega_0=\sqrt{K_3+\frac{K_1K_2}{K_1+K_2}\over M} \tag{23}$$

$$\omega_s=\sqrt{\frac{K_s}{M_s}} \tag{24}$$

$$\omega_{c1}=\sqrt{\frac{1}{2}\left(\begin{array}{l}\dfrac{K_2+K_3}{M}+\dfrac{K_1+K_2+K_s}{M_s}\\ -\sqrt{\left(\dfrac{K_2+K_3}{M}-\dfrac{K_1+K_2+K_s}{M_s}\right)^2+4\dfrac{K_2^2}{MM_s}}\end{array}\right)} \tag{25}$$

$$\omega_{c2}=\sqrt{\frac{1}{2}\left(\begin{array}{l}\dfrac{K_2+K_3}{M}+\dfrac{K_1+K_2+K_s}{M_s}\\ +\sqrt{\left(\dfrac{K_2+K_3}{M}-\dfrac{K_1+K_2+K_s}{M_s}\right)^2+4\dfrac{K_2^2}{MM_s}}\end{array}\right)} \tag{26}$$

Note that Eq. (17) is a frequency equation to obtain possible reverse full annular rub solutions. The normal contact force N can be evaluated as below

$$N=\mathrm{Re}(N)= \\ C_r\frac{-1}{1+\mu^2}\left(K_1+K_2\right)\frac{a_1(\omega)+a_2(\omega)+a_3(\omega)+\mu\left[a_4(\omega)+a_5(\omega)\right]}{\left[a_6(\omega)\right]^2+\left[a_7(\omega)\right]^2} \tag{27}$$

where

$$a_6(\omega)=\left(\omega^2-\omega_{c1}^2\right)\left(\omega^2-\omega_{c2}^2\right)-\frac{D}{M}\omega\left(\frac{D_s}{M_s}\omega+\omega_s^2\eta_s\right) \tag{28}$$

$$a_7(\omega)=\left(\omega^2-\frac{K_2+K_3}{M}\right)\left(\frac{D_s}{M_s}\omega+\omega_s^2\eta_s\right) \\ +\frac{D}{M}\omega\left(\omega^2-\frac{K_1+K_2+K_s}{M_s}\right) \tag{29}$$

Substituting Eq. (17) into Eq. (27) yields

$$N=-\left(C_r\frac{K_1+K_2}{\mu}\right)\frac{a_4(\omega)+a_5(\omega)}{\left[a_6(\omega)\right]^2+\left[a_7(\omega)\right]^2} \tag{30}$$

Note that the normal contact force must be positive ($N>0$) for any possible solutions obtained from the frequency equation Eq. (17). $N>0$ is a necessary condition for reverse rub to occur. If reverse rub frequency solution cannot make the contact force N positive, possibility of reverse rub is ruled out.

After obtaining the valid reverse rub frequency ω, the corresponding amplitudes and relative phase angles on the rotor and the seal can be evaluated. Absolute phase angles are dependent on the initial condition and defined starting time, but relative phase angles among ρ, ρ_r, ρ_s can be obtained.

From Eqs. (9) to (12), amplitudes and relative phase angles can be given by

$$A=C_r\left|\frac{K_2R_s(\omega)}{R(\omega)R_s(\omega)-K_2^2+\left(K_1+K_2\right)R(\omega)}\right| \tag{31}$$

$$A_re^{j(\alpha_r-\alpha)}=C_r\left|\frac{R_s(\omega)}{R(\omega)R_s(\omega)-K_2^2+\left(K_1+K_2\right)R(\omega)}\right|R(\omega) \tag{32}$$

$$A_se^{j(\alpha_s-\alpha)}=A\frac{K_2^2-\left(K_1+K_2\right)R(\omega)}{K_2R_s(\omega)} \tag{33}$$

where $R(\omega)$ and $R_s(\omega)$ are evaluated by using Eqs. (13) and (14) with the valid reverse rub frequency ω.

SIMULATION AND DISCUSSION OF ANALYTICAL RESULTS

Without detailed evaluation of reverse rub calculations from the above equations, some conclusions can be drawn based on the necessary condition of positive normal contact force ($N > 0$). Looking into expressions of Eqs. (21) and (22) clearly indicates that a valid solution of reverse rub frequency must be negative ($\omega < 0$) in order to make Eq. (30) positive, assuming μ is positive.

Should reverse rub frequency ω (< 0) be high enough to make slip velocity $v_{slip} < 0$, friction factor μ would be negative. In rolling cases without slippage, should the frictional force change its assumed direction due to high value of ω (< 0) to become in the same direction as rotor speed, friction factor μ would also be negative. The necessary condition of positive normal contact force expressed in Eq. (30) would then require $a_4(\omega) + a_5(\omega) > 0$, which is basically equivalent to $\omega > 0$. This would be contradictory to the assumed reverse rub with $\omega < 0$. Therefore, for reverse rub, friction factor μ must be positive as assumed, i.e., the frictional force μN acting on the rotor must be in the opposite direction to rotor speed Ω. This conclusion holds true by modeling the contact part as either the less stiff seal only or the whole stator. Thus, for reverse full annular rub, the following expressions are valid:

$$\mu > 0 \tag{34}$$

$$v_{slip} \geq 0 \tag{35}$$

and

$$|\omega| \leq \frac{r}{C_r}\Omega \tag{36}$$

where "=" holds for the motion of rolling without slippage, i.e., dry-friction whirl.

Parameters for analytical simulation are selected to be close to the experimental setup that will be discussed later in the paper. The model used for this analysis has a rotor mass M = 1 kg, and seal mass M_s =0.1 kg with stiffness K_1=15 kN/m, K_2= 250 kN/m, K_3= 25 kN/m, and K_s= 25 kN/m. Thus, the four natural frequency expressions, given by Eqs. (23) to (26), can be calculated as $\omega_0 = 1889$ cpm (cycle per minute, rotor natural frequency without rubbing contact), $\omega_s = 15099$ cpm (seal natural frequency), $\omega_{c1} = 3698$ cpm (the lower rotor/seal coupled natural frequency), and $\omega_{c2} = 21932$ cpm (the higher rotor/seal coupled natural frequency).

With the above parameters, Fig. 2 shows valid reverse full annular rub results by varying friction factor μ at rotor damping D=10 N m/s (damping ratio $\zeta = \frac{D}{2M\omega_0} = 0.025$), seal damping D_s=10 N m/s (damping ratio $\zeta_s = \frac{D_s}{2M_s\omega_s} = 0.032$), and seal structure damping factor η_s=0.01. The valid solutions exist with friction factor μ= 0.1083 or above only, when a positive normal contact force N is available. Therefore, dry-friction whirl/whip-free region exists with friction factor μ < 0.1083, as shown in the left area of position O in Fig. 2 (a). As μ increases from this value, there are two solutions corresponding to the same μ. Note that the solutions apply to both whirl and whip. In the case of whirl where slip velocity is zero, the frictional force μN is generally less than $\mu_{slip}N$, or in the other word the resultant contact force is within friction angle $\tan^{-1}(\mu_{slip})$. And in the case of whip where slip velocity is greater than zero, the frictional force μN is approximately equal to $\mu_{slip}N$, i.e., $\mu=\mu_{slip}$ as marked by line AB in Fig. 2 (a). Based on observed experimental results [7, 11], dry-friction whirl ranges from position A to O, and then from position O to B, as rotor speed increases. At position B, dry-friction whip starts and maintains with the same frequency, the same normal contact and frictional forces, and amplitude even though rotor speed keeps increasing.

Figure 3 shows valid reverse full annular rub results by varying rotor damping ratio ζ ($=\frac{D}{2M\omega_0}$) at friction factor μ = 0.2 while keeping other parameters the same as in Fig. 2. In contrast to the effect of friction factor μ in Fig. 2, the valid solutions exist with rotor damping ratio ζ = 0.0465 or below when a positive normal contact force N can be found, as shown in Fig. 3. Clearly, dry-friction whirl/whip-free region also exists with rotor damping ratio ζ > 0.0465, as shown in the right area in Fig. 3. As ζ decreases from this value, there are two solutions corresponding to the same ζ. Note that Fig. 3 can be used to see the effect of rotor damping in cases where μ remains constant, such as dry-friction whip ($\mu = \mu_{slip}$) or dry-friction whirl at a constant speed.

Dry-friction whirl/whip frequency $|\omega|$, as shown in Figs. 2 and 3, is always above ω_0 (rotor natural frequency without rubbing contact), but below ω_{c1} (the lower rotor/seal coupled natural frequency). The amplitudes and rubbing contact force are proportional to the seal clearance. Though mathematically at maximum 8 possible solutions could occur from the frequency equation Eq. (17), only up to 2 solutions can yield the positive contact force in the normal direction. It is believed that position B, instead of position A, corresponds to whip condition [2].

To clearly obtain a scenario of whirl/whip for known slip friction factor μ_{slip} and rotor radius–to–radial-clearance ratio r/C_r, as well as other parameters, Fig. 4 presents relevant results in terms of rotor speed. The slip friction factor μ_{slip} and rotor radius–to–radial-clearance ratio r/C_r are set to be 0.2 and 40, respectively. The shaft diameter is set to be 10 mm. The rotor damping ratio ζ remains to be 0.025, and other parameters are the same as in Fig. 2. Eq. (36) is used to distinguish between whirl and whip. Possible dry-friction whirl ranges from position A to B, i.e., for rotor speed Ω from 54 rpm to 85 rpm. If the whirl occurs within this range as rotor speed increases, friction factor μ will have to decrease from position A to O, followed by an increase from position O to B, though the frictional force μN tends to increase all the time. The solution of whirl in the region AO cannot be ruled out from the current analysis. Whirl frequency linearly increases with rotor speed in the ratio r/C_r. Normal contact and frictional forces, as well as amplitudes also increase with rotor speed from position A to B during the whirl range. As rotor speed keeps increasing after position B, dry-friction whip develops with the constant reverse frequency, and the contact force and vibration amplitudes remain constant as well. The positions A and B are comparable to those in Black's paper [2].

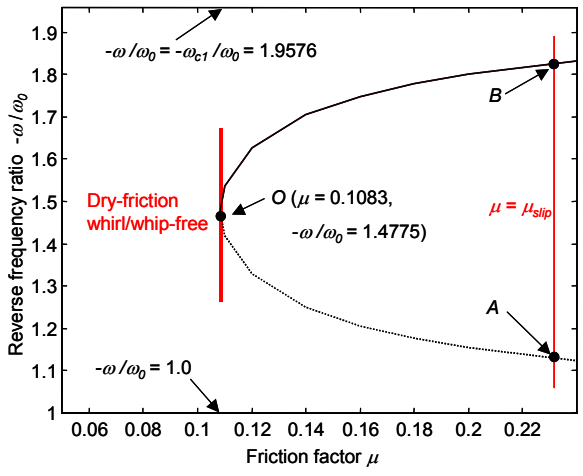

(*a*)

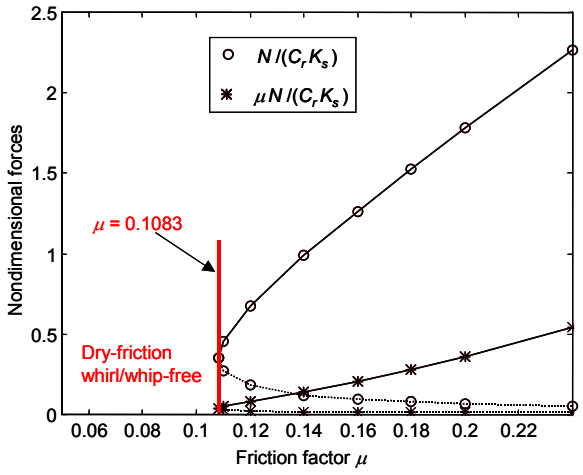

(*b*)

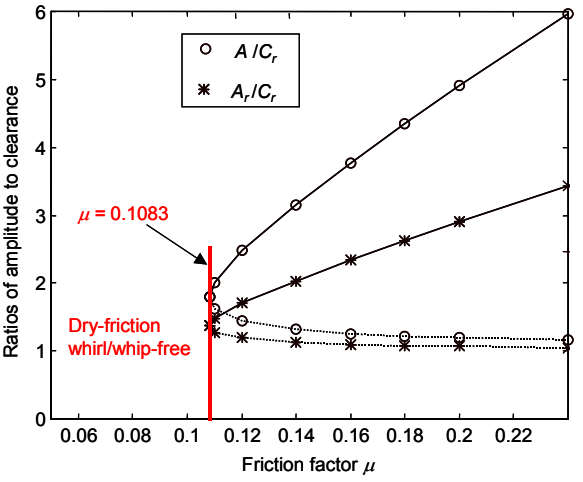

(*c*)

Figure 2. Valid reverse rub solutions with friction factor μ at D=D_s=10 N m/s, η_s=0.01; (*a*) reverse rub frequency ratio – ω/ω_0 ; *(b)*positive nondimensional normal contact force $N/(C_rK_s)$ and frictional force $\mu N/(C_rK_s)$; and (c) ratios of rotor amplitudes to clearance at rotor mass A/C_r and rubbing location A_r/C_r

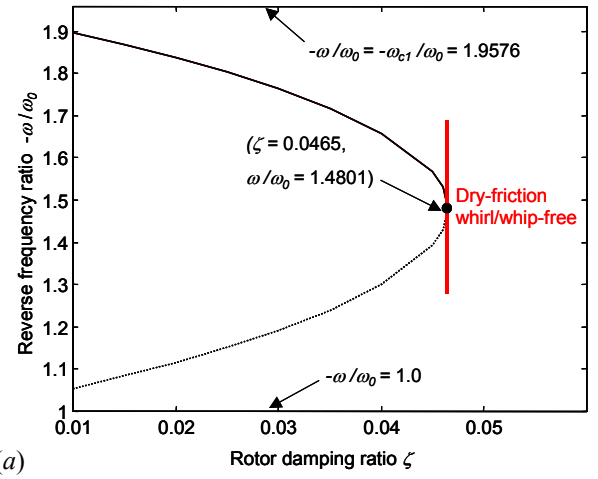

(*a*)

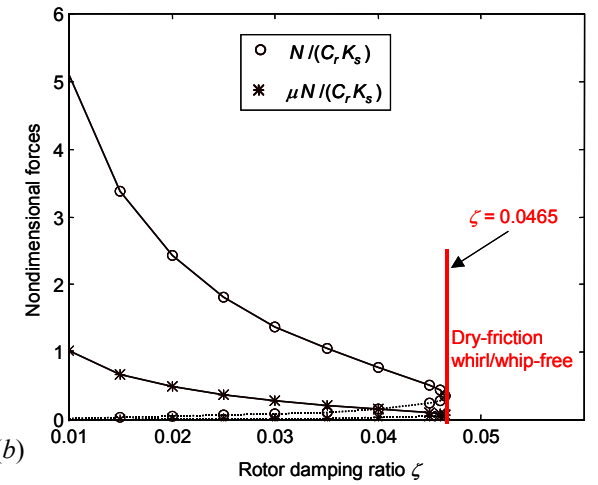

(*b*)

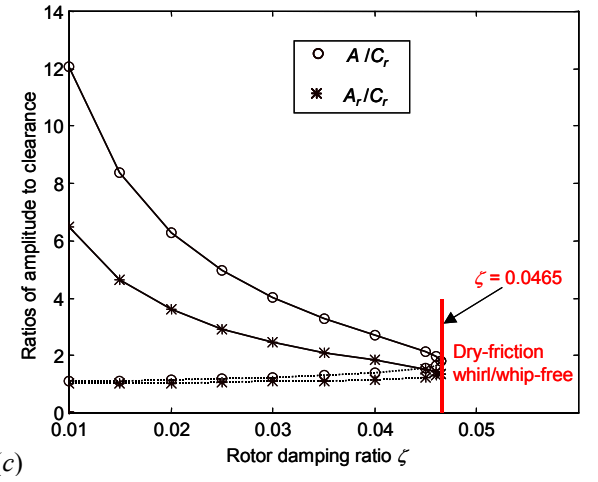

(*c*)

Figure 3. Valid reverse rub solutions with rotor damping ratio ζ at μ=0.2, D_s=10 N m/s, η_s=0.01; (*a*) reverse rub frequency ratio $-\omega/\omega_0$; *(b)*positive nondimensional normal contact force $N/(C_rK_s)$ and frictional force $\mu N/(C_rK_s)$; and (c) ratios of rotor amplitudes to clearance at rotor mass A/C_r and rubbing location A_r/C_r

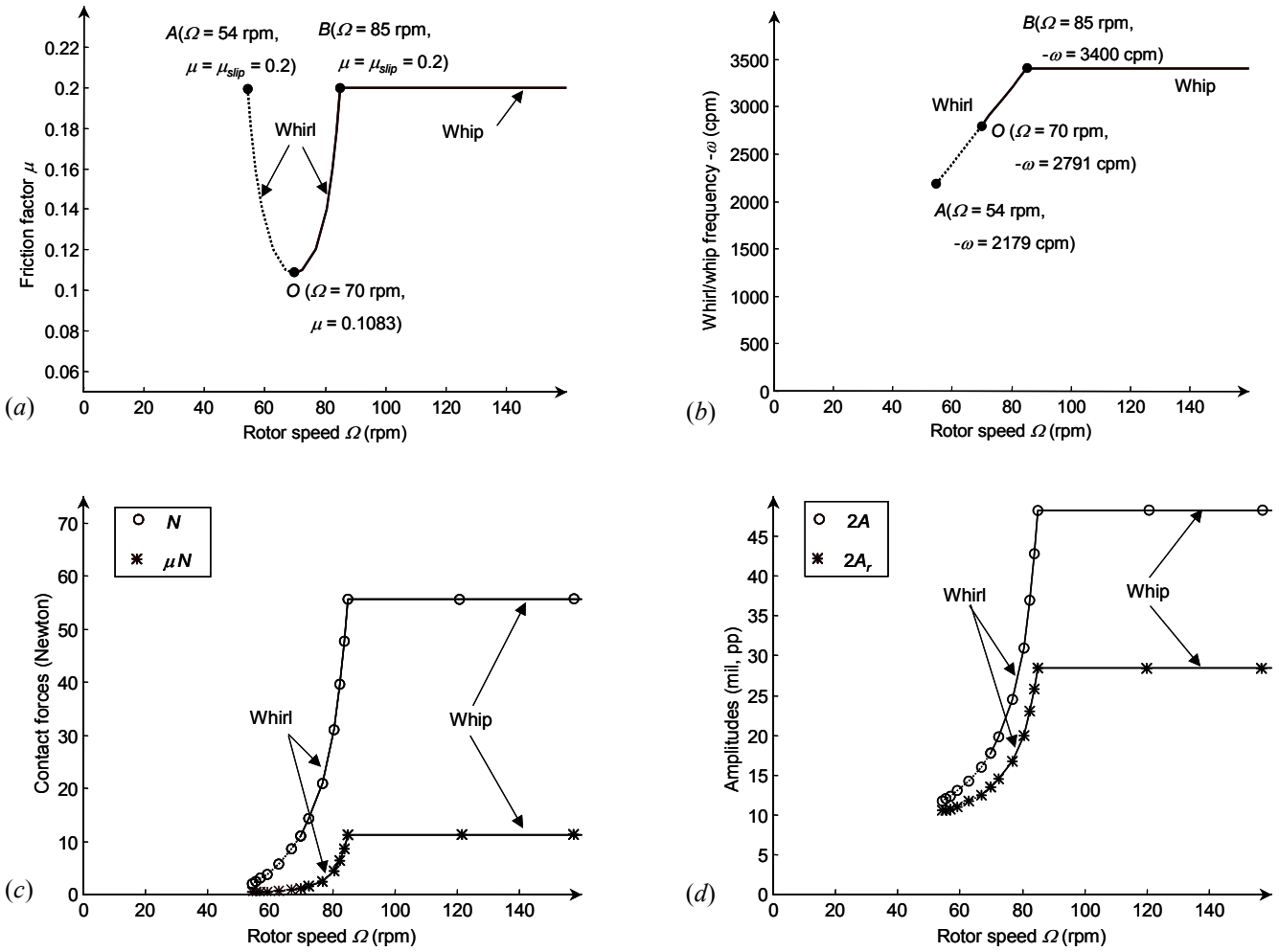

Figure 4. Valid reverse rub solutions in terms of rotor speed Ω at slip friction factor μ_{slip}=0.2 and rotor damping ratio ζ = 0.025 with rotor radius–to–radial-clearance ratio r/C_r=40 for 10 mm diameter shaft; (*a*) friction factor μ; (*b*) whirl/whip frequency; *(c)* normal contact force N and frictional force μN; and (*d*) rotor peak-to-peak amplitudes at rotor mass 2A and rubbing location 2A_r

MEASURED RESULTS

The current experimental study presents measured results that were not included in the earlier work [7] despite its similar setup. Figure 5 shows the experimental setup for reverse full annular rub, very close to the analytical model in Fig. 1. A steel shaft with diameter of 10 mm and length of 560 mm was supported by two brass bushing bearings and driven by a 75 W motor. A 0.8-kg disk was attached to the shaft. Seals used in experiments were either tightly assembled or flexibly fitted with an O-ring within the seal block. Teflon and bronze seals with diametral clearance varying from 0.25 to 1.0 mm were used. Radial probes were installed in both horizontal and vertical directions adjacent to the seal block as well as between the rotor mass and inboard bearing.

Yu et al. [7] shows that dry whip can be generated from forward synchronous rub due to high unbalance response. The current paper demonstrates the reverse full annular rub starting from a very low speed due to an impact and maintaining afterwards, as indicated in Fig. 6. At slow roll speed of about 262 rpm, reverse rub started due to an impact that made the shaft touch the seal surface, as shown in Fig. 6(a). The starting frequency was slightly below 2000 cpm, and appeared to be in the transition region from whirl to whip, as observed also by Childs and Bhattacharya [10]. As speed increased, the reverse full annular rub maintained, and its frequency was locked at around 2200 cpm. This constant frequency, as indicated by a waterfall plot in Fig. 6(b), clearly shows dry-friction whip, which is very destructive, especially at high shaft speed due to the corresponding high slip velocity.

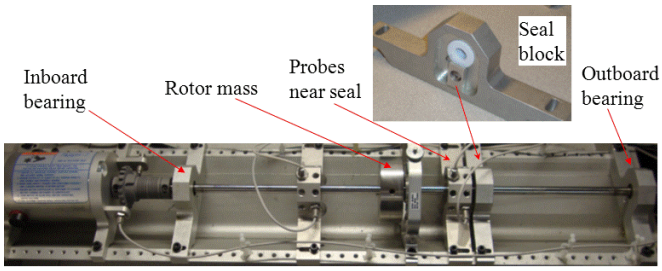

Figure 5. Rub experimental setup

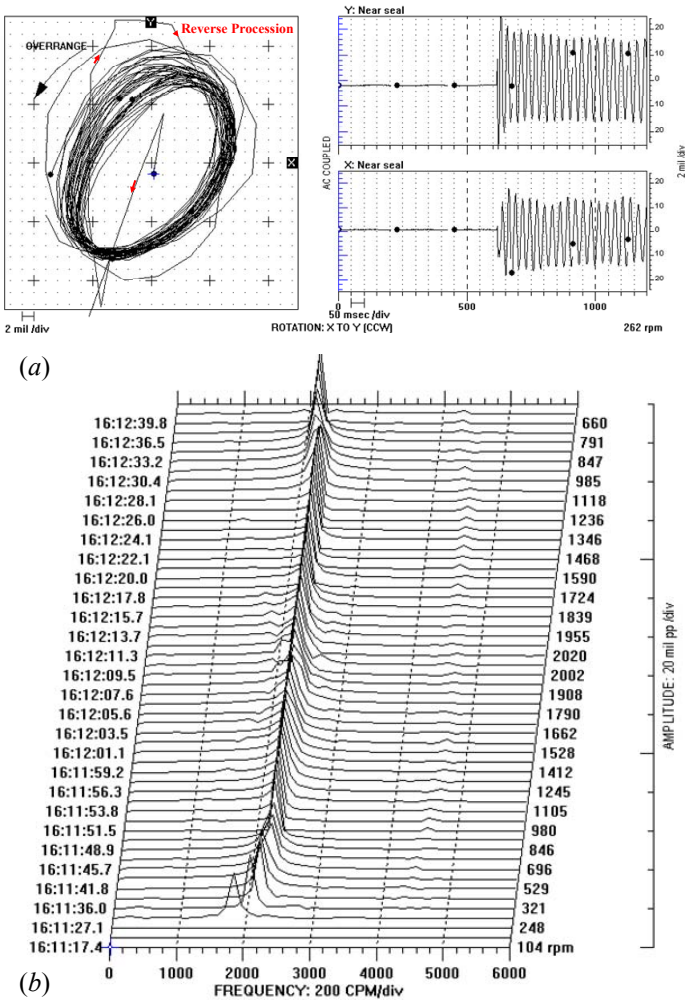

Figure 6. Reverse full annular rub (a) triggered at 262 rpm as shown in time base, and (b) waterfall plot measured by horizontal probe near seal

Comparisons were studied between calculated results from the analytical model and measured data from the experimental set up as shown in Fig. 5. The rotor mass and seal block locations are listed in Fig. 7. The rotor mass is M = 0.8 kg. The modulus of elasticity for this steel shaft is E=2×10^{11}Pa along with area moment of inertia I=πd^4/64 where shaft diameter d = 0.01m. Therefore, three stiffness values from the shaft are K_1'=3EI/[0.28^3-(0.28-0.171)^3] = 14.258 kN/m, K_2= 3EI/(0.28-0.171)^3=227.427 kN/m, and K_3'=3EI/(0.514-0.28)^3 =22.987 kN/m. Note that inboard/outboard bearing stiffness is K_b=1000 lb/in=175.126 kN/m. Thus, K_1= K_1' K_b/(K_1' +K_b)= 13.184 kN/m, and K_3= K_3' K_b/(K_3' +K_b). Test data without rubbing yielded the rotor damping D=10.2 N s/m. All these data matches the rotor peak response speed, which is close to the rotor natural frequency ω_0 =1933 cpm, without rubbing contact.

Four different seals, as shown in Fig. 8, were placed respectively within the seal block to observe their corresponding reverse rub frequencies and amplitudes. Seal 1 was tightly fitted without an O-ring within the seal block. The rest seals were fitted with an O-ring. Material of seals 1 to 3 was Teflon while seal 4 was made of brass. Their mass was easily obtained with a scale. The corresponding stiffness was

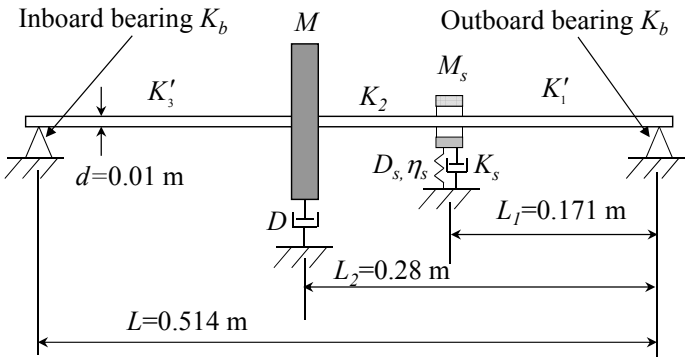

Figure 7. Diagram of experimental setup and distance of rotor mass and seal block relative to two bearings

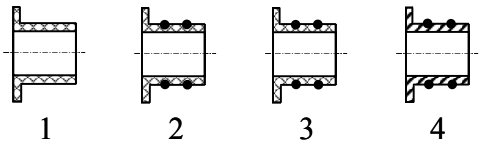

Figure 8. Four seals numbered from 1 to 4

computed through loading test. Its damping D_s was assumed to be the same as rotor damping D, and structural damping factor η_s was assumed as 0.01.

Table 1 shows comparison between measured and calculated dry whip results, which can be interpreted as the solution at position B in Fig.2 (a) or speed after position B in Fig. 4. Note that the rotor natural frequency ω_0 was about 1933 cpm without rubbing. The measured whip frequencies with different seals, however, were significantly dependent on seal stiffness. The calculated lower rotor/seal coupled natural frequency ω_{c1} was 4686, 3723, 3391, and 3386 cpm from seals 1 to 4, respectively. The corresponding measured whip frequencies were below these upper limits as indicated in Fig.2 (a), and turned out to be 4080, 3360, 2880, and 2880 cpm from seals 1 to 4, respectively. Measured whip amplitudes near the seal block were also proportional to the seal clearance, as indicated by Eq. (32), from around 25 mils, pp to over maximum range of 50 mils, pp when diametral seal clearance varied from 0.25 mm to 1.0 mm. Calculated dry-friction whip results are in good agreement with measured ones by selecting slip friction factor μ_{slip} as shown in Table 1. A lower value of μ_{slip} in the case of seal 1 was probably caused by relatively stiff contact surface without soft O-ring. The clearance on seal 1 was likely increased due to severe wear on its surface without soft O-ring, thus making the rotor amplitude higher than the calculated. The calculated normal contact forces are 54, 35, 53, and 35 N for cases in order with seals 1 to 4. These are corresponding to position B in Fig. 2 (a). The solution at position A with much lower contact forces and amplitudes, though satisfying the same equations with the same parameters, did not occur as whip in reality. Black [2] also ruled out the possibility of whip at position B.

Dry-friction whirl/whip was also reported in some real machines besides experiments. One case involves a high vibration issue on an anemometer at test stand. The shaft was running at around 400 rpm with a non-synchronous vibration

Table 1 Comparison between measured and calculated dry whip results

Seal No.	1	2	3	4
M_s (gram)	4.7	3.5	3.3	8.8
K_s (kN/m)	699	170	112	112
$2C_r$ (mm)	0.25	0.25	1.0	1.0
	Measured (Calculated)	Measured (Calculated)	Measured (Calculated)	Measured (Calculated)
μ_{slip}	(0.130)	(0.235)	(0.205)	(0.206)
- ω (cpm)	4080 (4079)	3360 (3362)	2880 (2881)	2880 (2880)
$2A_r$ (mil, pp)	25 (16)	27 (26)	>50 (77)	>50 (77)

component at around 1800 cpm measured by an accelerometer. This was suspected as dry-friction whip, though its reverse precession could not be confirmed by accelerometers.

CONCLUSIONS

Based on the current analytical model along with measured data in this paper, the following conclusions can be drawn:

(1) The current model can be used to analyze dry-friction whirl/whip phenomenon effectively. The model is close to the experimental setup, and allows for axial variation of rub contact position. The seal part, not the whole stator, is included in the model. The closed-form solution is obtained with the necessity of positive normal contact force, and can be applied to either seal or whole stator model.

(2) Up to two possible solutions exist in general to satisfy the condition of positive normal contact force. When slip friction factor μ_{slip} decreases to below a low value as indicated at position O in Fig.2, the rotor will not experience any dry-friction whirl/whip. For slip friction factor μ_{slip} that is along the vertical line AB in Fig.2, as rotor speed increase, whirl could start from position A to O, and then from position O to B while real friction factor μ varies. Though whirl from position O to B is more likely to occur than from position A to O, the latter case cannot be ruled out. At position B, whip starts when μ reaches μ_{slip}. As speed keeps increasing, whip frequency remains constant.

(3) Increasing rotor damping has the similar effect as decreasing friction factor. When the damping increases to above a high value as indicated in Fig.3, the rotor/seal system will be dry-friction whirl/whip-free. The two solutions can be interpreted as though they are located at upper and lower curves in the case of varying friction factor μ. The rotor damping effect on dry-friction whirl/whip was not discussed in Black's paper [2].

(4) Dry-friction whirl/whip frequency is always above the rotor natural frequency without rubbing contact, and below the lower rotor/seal coupled natural frequency. The vibration amplitudes and rubbing contact force are proportional to the seal clearance.

(5) It is proofed that the frictional force is always in the direction opposite to shaft speed for any reverse full annular rubs, even at very high shaft speed. Dry-friction whirl frequency is equal to the rotor speed times the ratio of rotor radius-to-radial-clearance while dry-whip frequency keeps constant and therefore is lower than this value as speed increases.

(6) Measured results are in good agreement with the analytically predicted whip results including frequency values and amplitudes by selecting slip friction factor μ_{slip}. For the same rotor in the experimental setup, values of seal stiffness significantly affected whip frequencies, which indicates an appropriate model of using the seal part only, instead of the whole stator.

ACKNOWLEDGMENT

The author is grateful to General Electric for permission and support in publishing this paper.

NOMENCLATURE

A, α = whirl/whip amplitude (0-peak) and phase of rotor at lumped rotor mass

A_r, α_r = whirl/whip amplitude (0-peak) and phase of rotor at seal location

A_s, α_s = whirl/whip amplitude (0-peak) and phase of seal

C_r = radial clearance between the rotor and the seal

D = rotor damping

D_s = seal damping

E = modulus of elasticity for the shaft

I = area moment of inertia of the shaft

K_1 = stiffness between right bearing support and seal

K_2 = stiffness between seal location and rotor mass

K_3 = stiffness between rotor mass and left bearing support

K_b = bearing stiffness

K_s = seal stiffness

K_1' = part of stiffness K_1 that includes shaft only without considering bearing stiffness

K_3' = part of stiffness K_3 that includes shaft only without considering bearing stiffness

M = lumped rotor mass

M_s = seal mass

N = normal contact force

$R(\omega)$ = variable in terms of rotor parameters and possible whirl/whip frequency

$R_s(\omega)$ = variable in terms of seal parameters and possible whirl/whip frequency

$a_i(\omega)$ = variable in terms of rotor/seal parameters and possible whirl/whip frequency (i varys from 1 to 5)

d = shaft diameter

h = center of mass eccentricity

t = time

v_{slip} = slip velocity of the rotor surface relative to the seal

Ω = shaft speed

ω = whirl/whip frequency (negative values)

ω_0 = rotor namtural frequency without rubbing contact

ω_s = seal namtural frequency

ω_{c1} = the lower rotor/seal coupled namtural frequency

ω_{c2} = the higher rotor/seal coupled namtural frequency

$\zeta = \dfrac{D}{2M\omega_0}$, rotor damping ratio

$\zeta_s = \dfrac{D_s}{2M_s\omega_s}$, seal damping ratio

μ = friction factor (varying without slippage, and $\leq \mu_{slip}$)

μ_{slip} = slip friction factor (almost constant)

$\rho = x + jy$, rotor displacement at lumped mass location

$\rho_r = x_r + jy_r$, rotor displacement at seal location

$\rho_s = x_s + jy_s$, seal displacement

η_s = seal structural damping

REFERENCES

[1] Black, H. F. 1967, "Synchronous Whirling of a Shaft Within a Radially Flexible Annulus Having Small Radial Clearance," IMechE Paper No. 4, **18** (65), pp. 29–37.

[2] Black, H., 1968, "Interaction of a Whirling Rotor With a Vibrating Stator Across a Clearance Annulus," J. Mech. Eng. Sci., **10**(1), pp. 1–12.

[3] Crandall, S., 1990, "From Whirl to Whip in Rotordynamics," IFToMM 3rd Int. Conf. on Rotordynamics, Lyon, France, pp. 19-26.

[4] Crandall, S. H., and Lingener, A., 1990, "Backward Whirl Due to Rotor-Stator Contact," *Proc. of XII Intl. Conf. Nonlinear Oscillations*, Sept. 2–7, Krakow.

[5] Lingener, A., 1990, "Experimental Investigation of Reverse Whirl of a Flexible Rotor," *Transactions, IFToMM 3rd International Conference on Rotordynamics*, Lyon, France, pp. 19–26.

[6] Childs, D.W., 1993, *Turbomachinery Rotordynamics: Phenomena, Modeling, and Analysis,* John Wiley & Sons, New York.

[7] Yu, J. J., Goldman, P., Bently, D.E., and Muszynska A., 2002, "Rotor/Seal Experimental and Analytical Study on Full Annular Rub," ASME J. Eng. Gas Turbines Power, **124**, pp.340-350.

[8] Bently, D. E., Yu, J. J., Goldman, P., and Muszynska, A., 2002, "Full Annular Rub in Mechanical Seals, Part I: Experimental Results," Int. J. Rotating Mach., **8**, pp. 319–328.

[9] Bently, D.E., Goldman, P., and Yu, J. J, 2002, "Full Annular Rub in Mechanical Seals, Part II: Analytical Study," Int. J. Rotating Mach., **8**, pp. 329-336.

[10] Childs, D. W., and Bhattacharya, A., 2007, "Prediction of Dry-Friction Whirl and Whip Between a Rotor and a Stator," ASME J. Vibr. Acoust., **129**, pp.355–362.

[11] Wilkes, J.C., Childs, D.W., Dyck B.J., and Phillips,S.G., 2010, "The Numerical and Experimental Characteristics of Multimode Dr-Friction Whip and Whirl," ASME J. Eng. Gas Turbines Power, **132**, p. 052503.